AD-A154 922 THE USE OF THE GLISTENING SURFACE CONCEPT IN ROUGH SURFACE SCATTERING(U) ROME AIR DEVELOPMENT CENTER GRIFFISS AFB NY R J PAPA ET AL. JUL 84 RADC-TR-84-159 1/1

UNCLASSIFIED F/G 17/9 NL

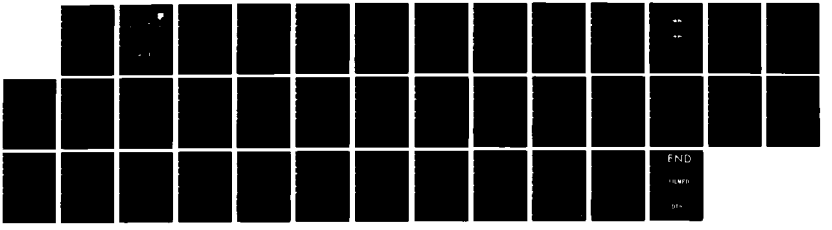

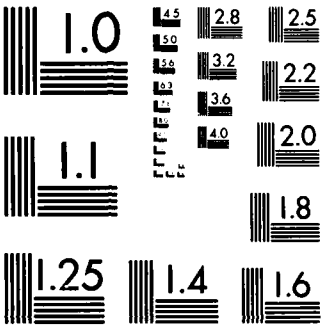

RADC-TR-84-159
In-House Report
July 1984

THE USE OF THE GLISTENING SURFACE CONCEPT IN ROUGH SURFACE SCATTERING

Robert J. Papa
John F. Lennon
Richard L. Taylor

ROME AIR DEVELOPMENT CENTER
Air Force Systems Command
Griffiss Air Force Base, NY 13441

This report has been reviewed by the RADC Public Affairs Office (PA) and is releasable to the National Technical Information Service (NTIS). At NTIS it will be releasable to the general public, including foreign nations.

RADC-TR-84-159 has been reviewed and is approved for publication.

APPROVED: Philipp Blacksmith

PHILIPP BLACKSMITH
Chief, EM Techniques Branch
Electromagnetic Sciences Division

APPROVED: Allan C. Schell

ALLAN C. SCHELL
Chief, Electromagnetic Sciences Division

FOR THE COMMANDER: John A. Ritz

JOHN A. RITZ
Acting Chief, Plans Office

If your address has changed or if you wish to be removed from the RADC mailing list, or if the addressee is no longer employed by your organization, please notify RADC (EECT) Hanscom AFB MA 01731. This will assist us in maintaining a current mailing list.

Do not return copies of this report unless contractual obligations or notices on a specific document requires that it be returned.

Unclassified
SECURITY CLASSIFICATION OF THIS PAGE

REPORT DOCUMENTATION PAGE

1a. REPORT SECURITY CLASSIFICATION Unclassified	1b. RESTRICTIVE MARKINGS
2a. SECURITY CLASSIFICATION AUTHORITY	3. DISTRIBUTION/AVAILABILITY OF REPORT Approved for public release; distribution unlimited.
2b. DECLASSIFICATION/DOWNGRADING SCHEDULE	
4. PERFORMING ORGANIZATION REPORT NUMBER(S) RADC-TR-84-159	5. MONITORING ORGANIZATION REPORT NUMBER(S)
6a. NAME OF PERFORMING ORGANIZATION Rome Air Development Center 6b. OFFICE SYMBOL (If applicable) EECT	7a. NAME OF MONITORING ORGANIZATION Rome Air Development (EECT)
6c. ADDRESS (City, State and ZIP Code) Hanscom AFB Massachusetts 01731	7b. ADDRESS (City, State and ZIP Code) Hanscom AFB Massachusetts 01731
8a. NAME OF FUNDING/SPONSORING ORGANIZATION Rome Air Development Center 8b. OFFICE SYMBOL (If applicable) EECT	9. PROCUREMENT INSTRUMENT IDENTIFICATION NUMBER
8c. ADDRESS (City, State and ZIP Code) Hanscom AFB Massachusetts 01731	10. SOURCE OF FUNDING NOS. PROGRAM ELEMENT NO.: 61102F PROJECT NO.: 2305 TASK NO.: J4 WORK UNIT NO.: 07
11. TITLE (Include Security Classification) The Use of the Glistening Surface (Contd)	
12. PERSONAL AUTHOR(S) Papa, Robert J.; Lennon, John F.; Taylor, Richard L.	
13a. TYPE OF REPORT In-House 13b. TIME COVERED FROM 6/83 TO 6/84	14. DATE OF REPORT (Yr., Mo., Day) 1984 July 15. PAGE COUNT 35
16 SUPPLEMENTARY NOTATION	

17 COSATI CODES			18 SUBJECT TERMS (Continue on reverse if necessary and identify by block number)
FIELD	GROUP	SUB GR	Radar clutter, Terrain scattering, Radar multipath.
Physics	20	14	
Det	17	09	

19. ABSTRACT (Continue on reverse if necessary and identify by block number)

Calculations of diffuse power scattered from a rough surface have typically used the concept of a glistening surface over which a centerline-varying surface cross section is integrated. The usual form of that surface is derived for relatively smooth surfaces and contains several other constraints that are not always evident. In this report, we will address the limitations on this definition and several alternative forms that are less restrictive. We will compare them with a more realistic solution in which the azimuthal variation in the surface cross section is taken into account and the integration is across the entire signal footprint on the surface.

The standard scattering surface dimensions are determined under constraints on both the antenna heights and the surface width. In the report, we analyze the effect of removing those constraints. In addition, we consider a second formulation in which one of the antenna terminals of the bistatic system is considered to be sufficiently distant so that it is treated as being at infinity. We examine the different boundary values for the (Contd)

20 DISTRIBUTION/AVAILABILITY OF ABSTRACT UNCLASSIFIED/UNLIMITED ☒ SAME AS RPT ☐ DTIC USERS ☐	21 ABSTRACT SECURITY CLASSIFICATION Unclassified
22a NAME OF RESPONSIBLE INDIVIDUAL Robert J. Papa	22b TELEPHONE NUMBER (Include Area Code) (617) 861-3735 22c OFFICE SYMBOL EECT

DD FORM 1473, 83 APR EDITION OF 1 JAN 73 IS OBSOLETE

Unclassified
SECURITY CLASSIFICATION OF THIS PAGE

Block 11 (Contd)

Concept in Rough Surface Scattering

Sigma deg.

Block 19 (Contd)

glistening surface based on these different assumptions and compare the resultant scattered power levels with the azimuthally varying cross section results.

One of the most important conclusions is that the use of the centerline normalized cross section models can lead to calculated diffuse power levels that are in disagreement with the results for the more exact solution in which both the azimuthal variation in σ^0 is accounted for and the integration is always across the entire radar footprint rather than a calculated glistening surface width. Need keywords include: sea 147?

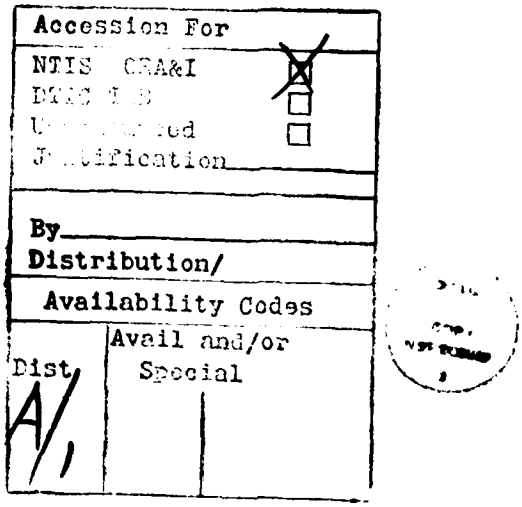

Contents

Illustrations

Illustrations

Tables

The Use of the Glistening Surface Concept in Rough Surface Scattering

1. INTRODUCTION

The scattering of electromagnetic waves from rough terrains depends on the characteristics of the rough surface.[1,2,3,4,5,6] The rough surface may be defined in terms of the statistical distribution of heights, their degree of correlation (T is the surface correlation length), the variance of heights σ^2, and the complex dielectric constant associated with a particular type of terrain. A number of theo-

(Received for publication 24 July 1984)

1. Papa, R.J., and Lennon, J.F. (1980) Electromagnetic scattering from rough surfaces based on statistical characterization of the terrain, International Radio Science Symposium (USRI), Quebec, Canada.

2. Papa, R.J., Lennon, J.F., and Taylor, R.L. (1980) Electromagnetic Wave Scattering From Rough Terrain, RADC-TR-80-300, AD A098939.

3. Papa, R.J., Lennon, J.F., and Taylor, R.L. (1982) The Need for an Expanded Definition of Glistening Surface, RADC-TR-82-271, AD A130431.

4. Papa, R.J., and Lennon, J.F. (1983) Investigation of backscatter from an uneven, rough surface, International Radio Science Symposium (URSI), Houston, Texas.

5. Papa, R.J., Lennon, J.F., and Taylor, R.L. (1982) Further Considerations in Models of Rough Surface Scattering, RADC-TR-82-326, AD A130424.

6. Papa, R.J., Lennon J.F., and Taylor, R.L. (1983) Multipath effects on an azimuthal monopulse system, Trans. IEEE on Aerospace and Electronic Systems, 585-597.

retical models describing rough surface scattering[7, 8, 9] relate these parameters to the normalized radar cross section of the rough surface. In these models, the surface area contributing to the scattering process (glistening surface) is defined in different forms. This report contains an analysis of different definitions of glistening surface and the constraints on their use for analyzing a bistatic radar system scattering signals from terrain. Three distinct situations will be discussed.

The first is the case where both antennas are at finite heights and a finite separation. Three subcases are discussed that depend upon the relation between the dimensions of the glistening surface and the antenna heights. Second, there is the case where one antenna is considered to be at infinity. Finally, there is the complete solution in which the azimuthally varying cross section is integrated over the entire signal footprint. This solution is used as a basis for comparison with the other results that have the more simplistic σ^o values in their integrations.

1.1 Background

In previous reports, [1, 2, 3, 4, 5, 6] we have explained that RADC/EEC has a continuing interest in improving the modeling of the scattering from rough surfaces. The investigations are devoted to two main topics: the characterization of the surface and the electromagnetic wave scattering. The models in those studies are based upon physical optics. A geometrical representation of scattering from a surface is shown in Figure 1. In the studies of this present report, the azimuthal and elevation patterns shown in Figure 2 correspond to the antenna located at the higher altitude. The lower antenna has an isotropic pattern, and the other system parameters are typical of those of the earlier reports.

The results of these investigations have implications for estimating radar system performance. It was shown earlier[5] that extended definitions of the glistening surface can give much more accurate diffuse power estimates than those given by the conventional radar engineering approach formulated by Barton and Ward.[10]

---

7. Beckmann, P., and Spizzichino, A. (1963) The Scattering of Electromagnetic Waves From Rough Surfaces, Macmillan Co., New York.
8. Ruck, G.T., Barrick, D.E., Stuart, W.D., and Krichbaum, C.K. (1970) Radar Cross Section Handbook, 2, Plenum Press, New York.
9. Long, N.W. (1975) Radar Reflectivity of Land and Sea, Lexington Books, Lexington, Mass.
10. Barton, D.K., and Ward, H.R. (1969) Handbook of Radar Measurement, Prentice-Hall, Inc., Englewood Cliffs, New Jersey.

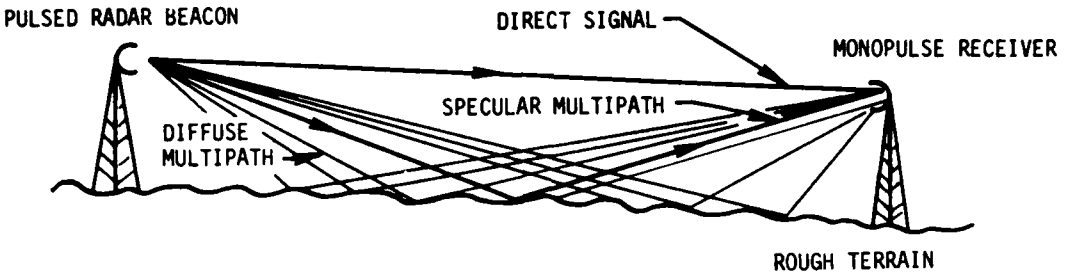

Figure 1. Schematic Representation of Rough Surface Scattering

1.2 Scope

The report discusses the basic limitations of the definitions and modifications that can be introduced when it is desired to apply the glistening surface models to cases that are not consistent with the original assumptions contained in the theory. The results obtained using different models are compared and discussed.

2. GLISTENING SURFACE DETERMINATION

In studies of scattering from rough surfaces, investigators have made wide use of the concept of glistening surface. The glistening surface is defined as that part of the rough surface that reflects a significant amount of the transmitted energy into the receiver for a given set of antenna positions.

Beckmann and Spizzichino[7] have derived a number of equations describing the boundaries of the glistening surface and the associated normalized rough surface scattering cross section. The different forms apply to a number of sets of conditions and configurations of the antennas. The form that has received wide usage is the one where it has been assumed that both the transmitting antenna height, H_A, and the receiver height, H_T, are small compared to the separation, d, between them (definition 1). There are a number of additional assumptions in the derivation of this result, and, since it has been applied extensively, it is worth examining the implications of these assumptions for the range of validity of the equations.

We begin by listing some general assumptions in their formalism. These include the following:

(1) It is assumed that the normalized rough surface scattering cross section σ° is derived under the conditions of physical optics;

(2) It is assumed that the surface heights can be described by a bivariate Gaussian or exponential statistical distribution; and

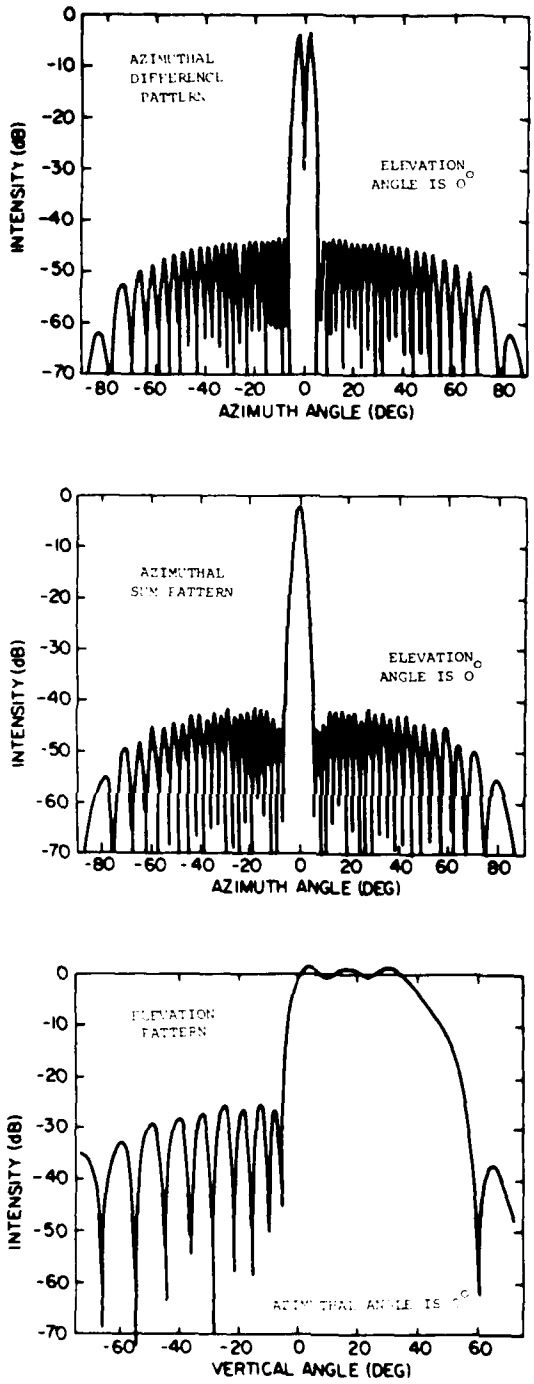

Figure 2. Azimuthal Plane Monopulse and Evaluation Plane Antenna Power Patterns

(3) It is assumed that the Rayleigh roughness parameter

$$\Sigma = [(2\pi\sigma/\lambda)(\cos\theta_i + \cos\theta_s)]$$

is much greater than one,

where σ = standard deviation in surface height,

λ = wavelength,

θ_i = angle of incidence,

and

θ_s = scattering angle (elevation).

The derivation of the boundary of the glistening surface then proceeds by considering the linear bisector of the angle, $\sphericalangle TPR$, in Figure 3. This bisector makes an angle, $\sphericalangle \beta$, with the vertical z-axis.

This angle β is related to the electromagnetics of the scattering:

$$\tan\beta = v_{xy}/v_z$$

where

$$v_{xy} = \sqrt{v_x^2 + v_y^2}$$

and v_x, v_y, v_z

are direction cosines of the difference vector $\vec{k}_d = \vec{k}_i - \vec{k}_r$, and $\vec{k}_i$ and $\vec{k}_r$ are the incident and reflected em wave vectors, respectively. If we define a roughness factor, $\text{Tan}\ \beta_o = (2\sigma/T)$ where σ is the standard deviation of the surface heights and T is the surface correlation length, then we can express the normalized rough surface cross section σ^o as:

$$\sigma^o \propto \exp\{-\tan\beta/\tan\beta_o\} \qquad \text{(Bivariate exponential surface)}$$

and

$$\sigma^o \propto \exp\{-\tan^2\beta/\tan^2\beta_o\} \qquad \text{(Bivariate Gaussian surface)}$$

Thus, from the electromagnetics, we define the glistening surface as the region

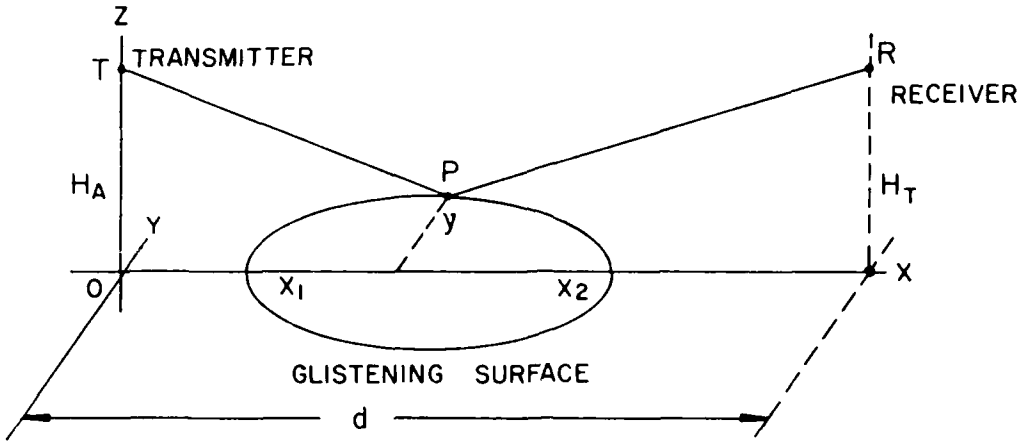

General Conditions for Arbitrary Point P on the Boundary

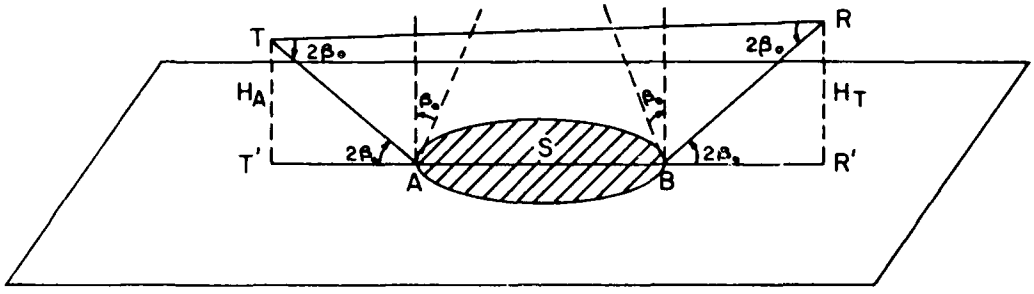

Special Conditions for Points A and B on X Coordinate Axis

Figure 3. Standard Glistening Surface Geometrical Representations: (a) Arbitrary Boundary Point, and (b) Axial End Points

where $|\beta \leq |\beta_o$, which is equivalent to the region for which the scattered power is equal to or greater than 1/e of its maximum.

Under the condition that H_A and $H_T \ll d$, the x-axial distances from the two antennas to the ends of the glistening surface are (Figure 3):

$$L_1 = TA = H_A \cot 2\beta_o \text{ and } L_2 = RB = H_T \cot 2\beta_o.$$

Next, by expressing the direction cosines of this bisector as a linear combination of the direction cosines of the lines PT and PR, and using the normalization condition on the direction cosines, it is possible to derive the equation for the

$$E = (X_1^2 + H_A^2)$$

This is not a convenient form for general application because iterative procedures have to be used to solve for the width. However, we can use it here to evaluate the effects in some specific instances. This will allow us to see how including the complete azimuthal angular dependence affects the extent of the glistening surface width.

The results for roughness levels where $\frac{1}{2}\beta_o < \pi/4$ are not surprising. The width values using the assumptions of the standard definition are small compared with the separations (x_1, x_2). Indeed, the iterated solutions including the complete azimuthal dependence are indistinguishable from the classical values. For larger roughnesses, though, where the widths are nonzero even at the antenna positions, we expected to see considerable differences. Figure 13, Figure 14, and Figure 15 show the results for σ^2 10 m^2 and T = 2 m at the three separations. This corresponds to $\frac{1}{2}\beta_o$ 72.45°. Even in these cases where the widths reach the order of several kilometers, the $2\beta_o$ standard and the iterated solutions are virtually identical at the two longer separations, and for the 9 km case they are similar except for distances less than twice the respective antenna heights. It is interesting to note that, at those distances, the standard width values exceed the iterated solution (which contains no assumptions on the relative smallness of the heights and widths). This is consistent with the results found when the height restriction was removed (see Figure 11). These figures also show that the modified ($d \to \infty$) results are similar to and even wider than the other values.

These discussions of the various width calculations have shown a number of interesting patterns. For larger roughness values, the standard $2\beta_o$ definition is in good agreement with the more complicated solutions of the less restrictive definitions. This holds true even for cases where the basic concepts implicit in the definition have been violated ($\frac{1}{2}\beta_o > 45°$). At smaller roughnesses (T = 200 m, 500 m), there is less agreement with the alternative definitions, particularly at the shorter separations where the $2\beta_o$ surface vanishes ($L_1 + L_2 > d$). There, the ($d \to \infty$) definition has a finite, relatively small surface. It should be noted that if the L_1 and L_2 constraints are neglected, the surface generated by the standard definition for these conditions is the same as the alternative result. This serves to confirm that, for those conditions, the assumptions implicit in the L_1 and L_2 determination have been violated as a result of the short separation distance. The alternative result is still valid even though the separation is not particularly infinite, compared with the 55 km or 90 km cases.

The point to emphasize here is that there is a clear distinction in the calculation of the two dimensions of the glistening surface and that the basic, simple definition can be used to give surfaces that agree with the more complicated formal-

fact that, for this roughness, L_1 and L_2 are small in the first definition. This introduces the additional complication that near either end of the surface, the condition that $H_A < x_1$, or $H_T < x_2$ is not satisfied. The question is what effect violating the condition has on the width of the surface. To resolve this, we show the results for a revised definition where the restriction is not included. Those width values are shown in the figures as crosses (+). At D = 30 NMI and D = 50 NMI, we see that the widths are only minimally altered by that assumption and that, once the distance has exceeded twice the height, the two surfaces are equivalent. At D = 5 NMI, the shapes are similar near the transmitter and show real differences only when $x_2 < H_T$, in which region the two widths are decreasing rapidly.

4. ANALYSIS

The discussions of these figures have pointed out how increasing roughness affects the first Beckmann and Spizzichino[7] definition results. As $\tan\beta_o$ increases, L_1 and L_2 decrease and the height to x-axis ratio condition is no longer satisfied along the entire surface. From Figure 10, it is clear that, as the roughness continues to increase, L_1 and $L_2 \rightarrow 0$. When $\not\triangleleft 2\beta_o \rightarrow 90°$, the entire geometric formalism breaks down. At even smaller angles, the condition that $y < x_1, x_2$ is becoming questionable. For instance, in Figure 12 we see that, even for $\not\triangleleft\beta_o \sim 30°$, there are points at which y is one-half the corresponding x distance.

This raises two questions. The first is how relaxing the y constraint affects the width. The second is what the considerations are when $\not\triangleleft\beta_o > \pi/4$. In the two preceding width derivations, the assumption that y is small simplified the angular component relationships. If we remove that condition, we can follow the same procedures as before, but the result is more complex. We arrive at a form:

$$y^2 = x_1 x_2 + \left[\frac{H_A^2}{2}\left(\frac{C + Y^2}{E + Y^2}\right)^{1/2} + \frac{H_T^2}{2}\left(\frac{E + Y^2}{C + Y^2}\right)^{1/2} + H_R H_T\right] TAN^2\beta_c$$

$$- \left(\frac{Y^2 + x_1^2}{2}\right)\left(\frac{C + Y^2}{E + Y^2}\right)^{1/2} - \left(\frac{Y^2 + x_2^2}{2}\right)\left(\frac{E + Y^2}{C + Y^2}\right)^{1/2}$$

where

$$C = (X_2^2 + H_T^2)$$

and

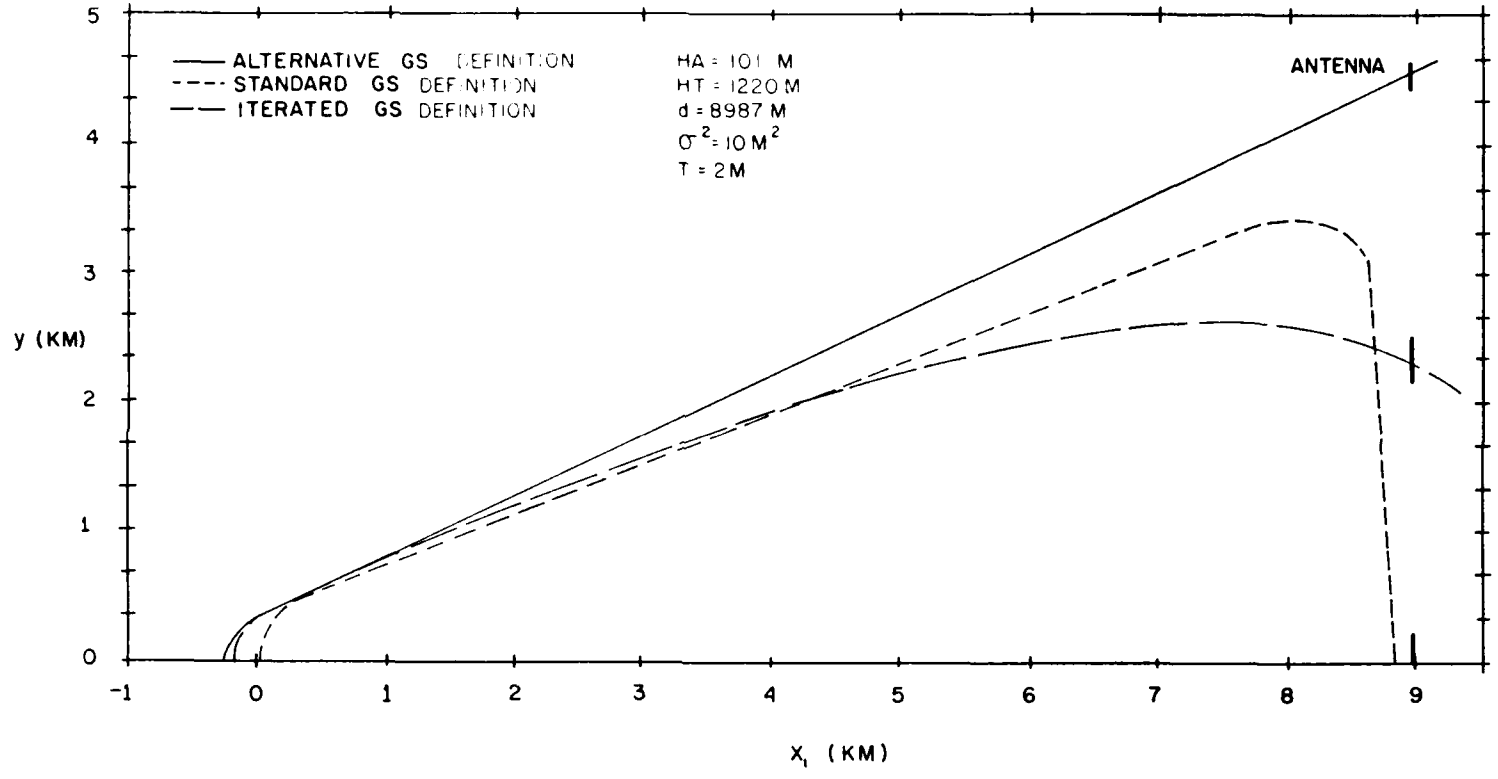

Figure 15. Glistening Surface Dimensions From Three Calculations, Short Antenna Separation (σ/T = 1.5)

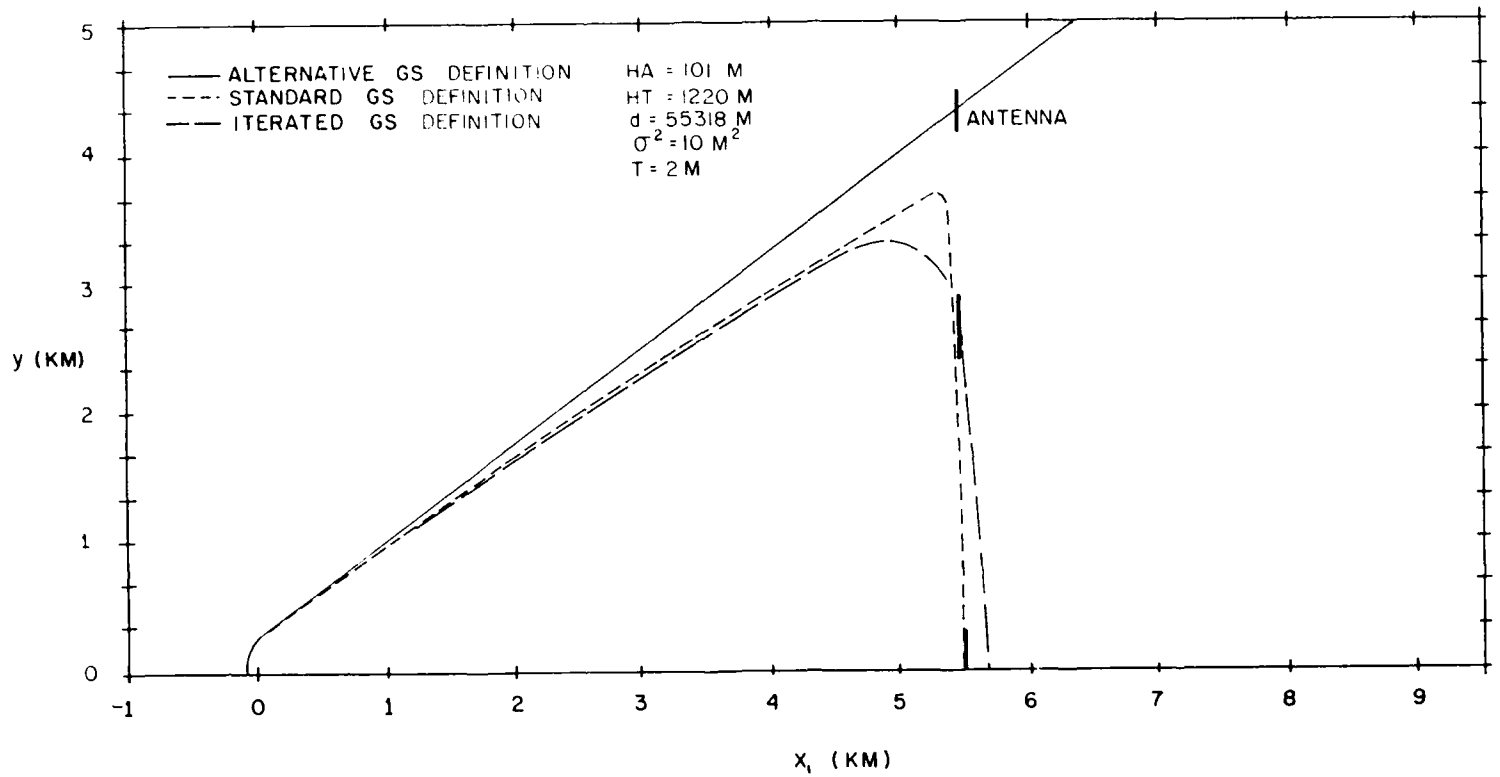

Figure 14. Glistening Surface Dimensions From Three Calculations, Intermediate Antenna Separation, Very Rough Surface (σ/T = 1.5)

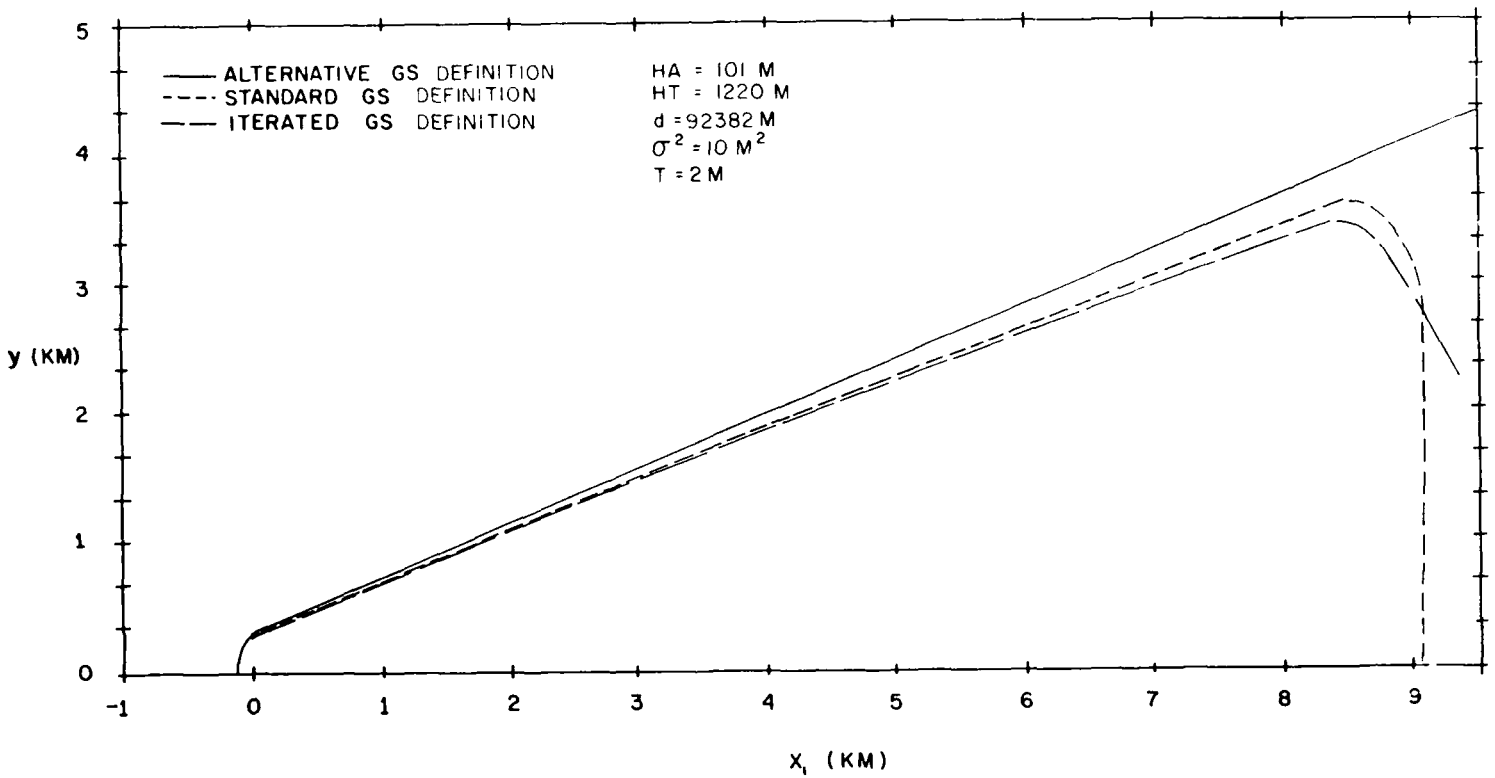

Figure 13. Glistening Surface Dimensions From Three Calculations, Large Antenna Separation, Very Rough Surface ($\sigma/T = 1.5$)

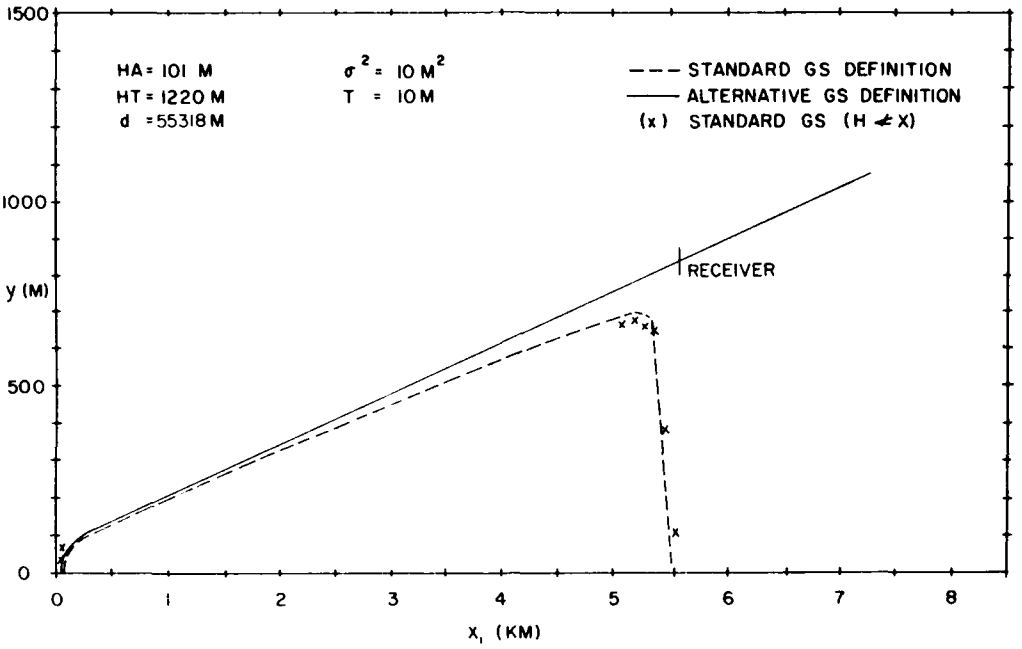

Figure 11. Glistening Surface Dimensions for Both Definitions, Intermediate Antenna Separation, Rough Surface ($\sigma/T = .33$)

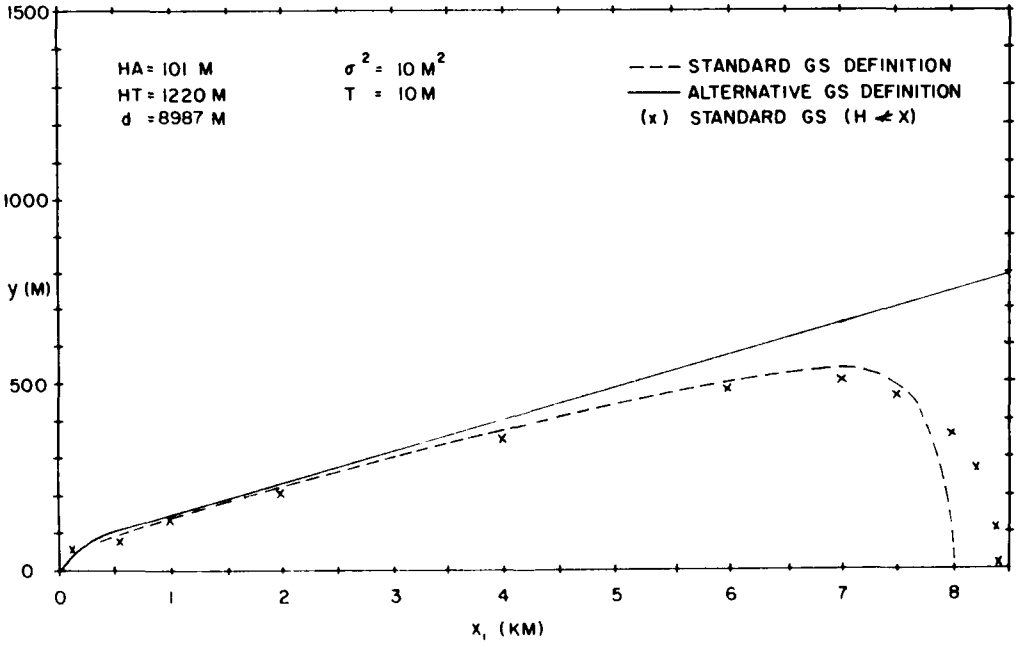

Figure 12. Glistening Surface Dimensions for Both Definitions, Short Antenna Separation, Rough Surface ($\sigma/T = .33$)

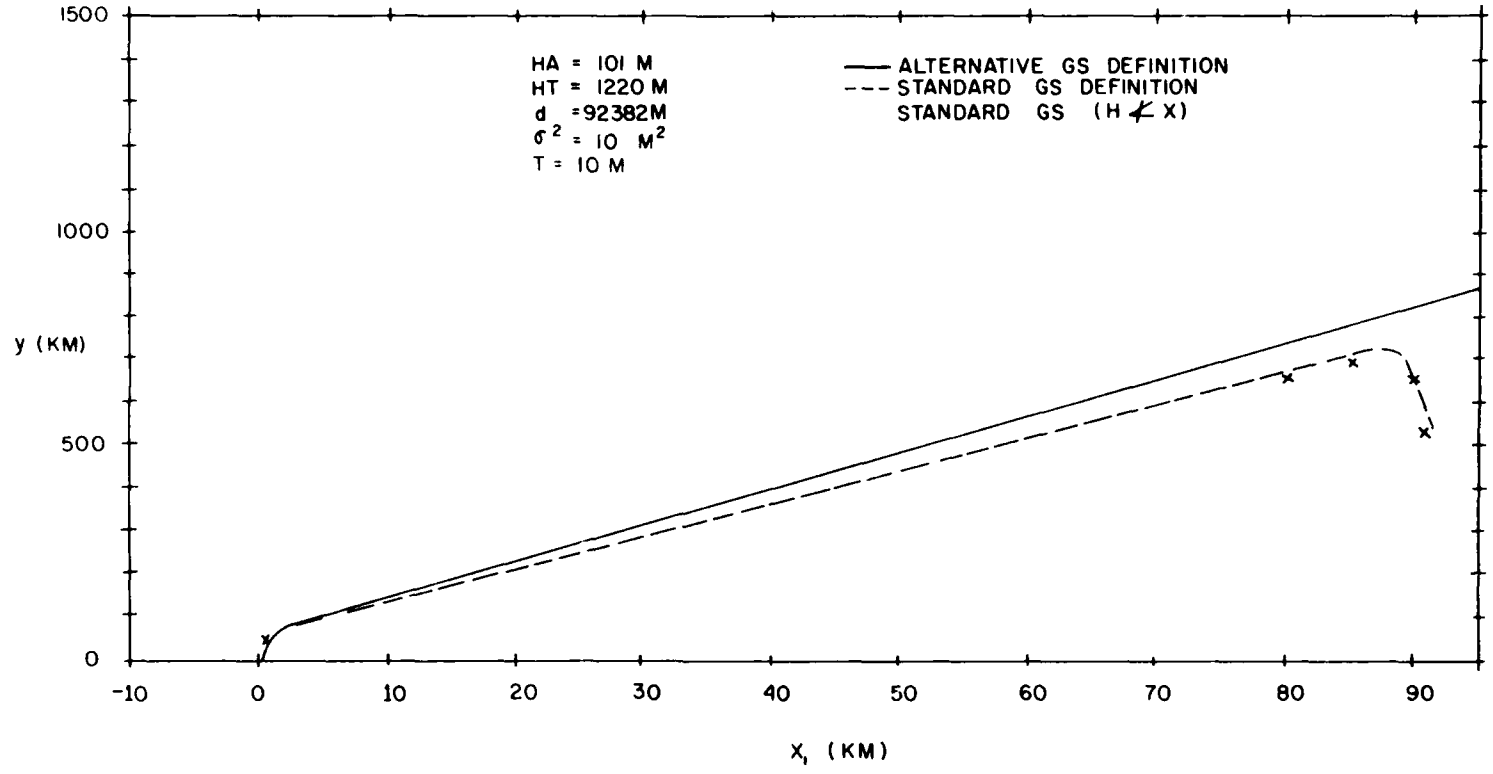

Figure 10. Glistening Surface Dimensions for Both Definitions, Large Antenna Separation, Rough Surface (σ/T = .33)

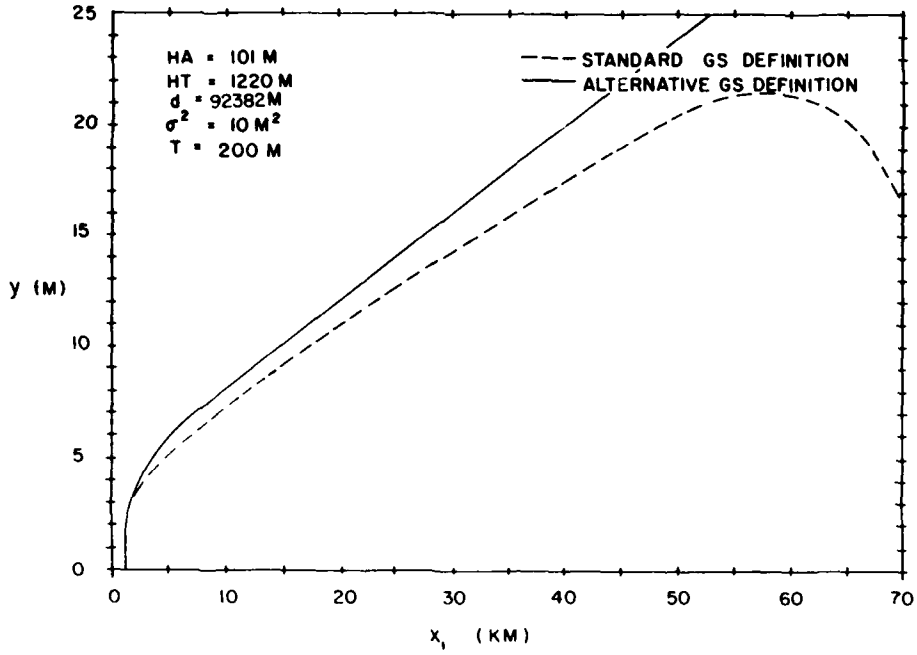

Figure 8. Glistening Surface Dimensions for Both Definitions, Large AnTenna Separation, Slightly Rougher Surface ($\sigma/T = .015$)

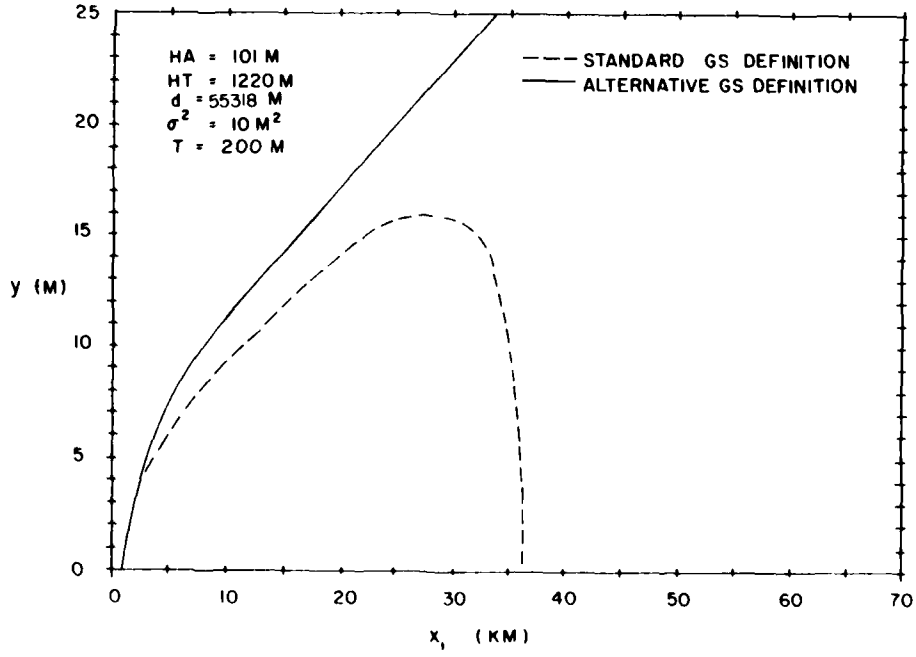

Figure 9. Glistening Surface Dimensions for Both Definitions, Intermediate Antenna Separation, Slightly Rougher Surface ($\sigma/T = .015$)

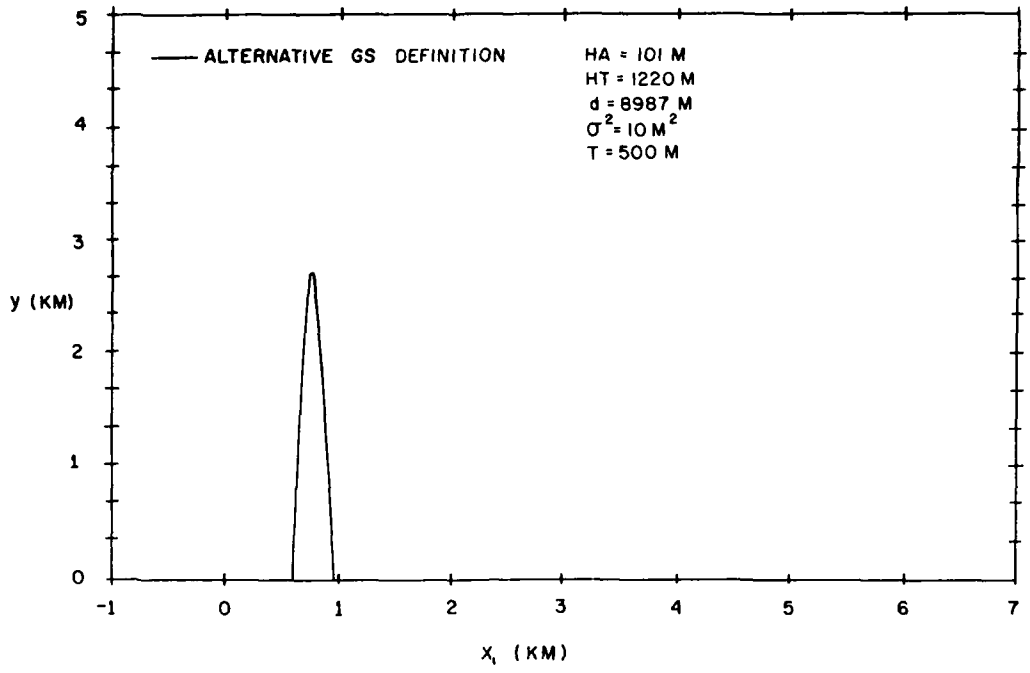

Figure 7. Glistening Surface Dimensions for the Alternative Definition, Short Antenna Separation, Smooth Surface (σ/T = .006)

Figure 8 and Figure 9 show the same comparisons for the case where $\sigma^2 = 10\,m^2$ and T = 200 m. This is a slightly rougher surface than before, but the condition that $h_1 < x_1$ and $h_2 < x_2$ is still valid over the extent of the glistening surfaces. As before, Figure 8 shows the results at D = 50 NMI, and Figure 9, at D = 30 NMI. The 5 NMI result isn't shown since the first definition again results in a nonexistent surface. The surface for the second definition is determined by the first condition and is a small finite region, as was the case in Figure 7. The second criterion of the second definition applies at D = 30 NMI and D = 50 NMI, and we have continuously increasing widths as x_1 increases. Since L_1 and L_2 are smaller in these instances, the first definition surfaces are longer and the agreement between the two models is quite reasonable for over half the separations. Again, the condition that $y < x_1, x_2$ is satisfied for the first definition.

Figure 10, Figure 11, and Figure 12 show the comparisons for a much rougher surface at the three selected separations. Here $\sigma^2 = 10\,m^2$ and T = 10 m. For these conditions, the surface of the second definition is always controlled by the second condition on $\frac{1}{2}\delta$, and hence continues to increase in width as x_1 increases. At all three separations, the two surfaces are quite similar. This is related to the

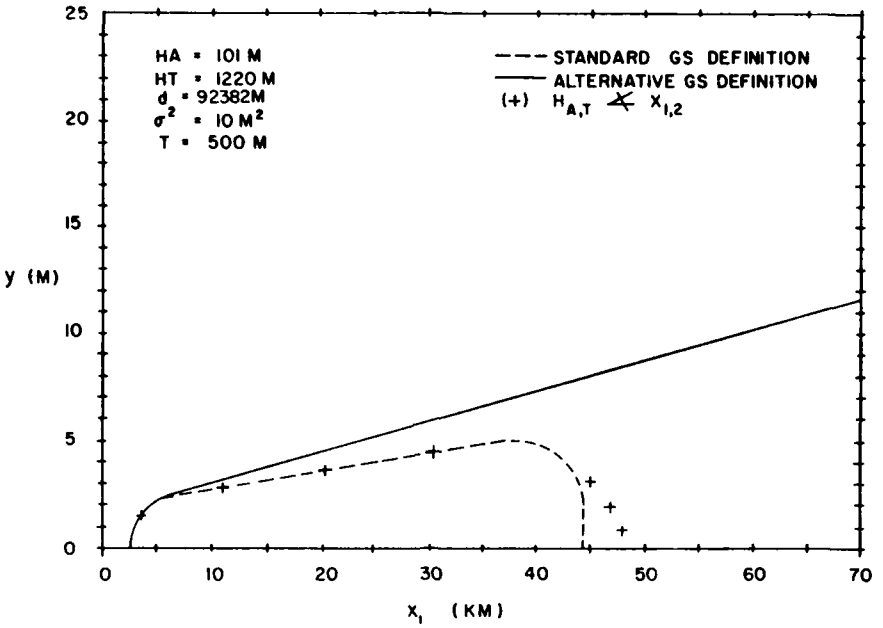

Figure 5. Glistening Surface Dimensions for Both Definitions, Large Antenna Separation, Smooth Surface ($\sigma/T = .006$)

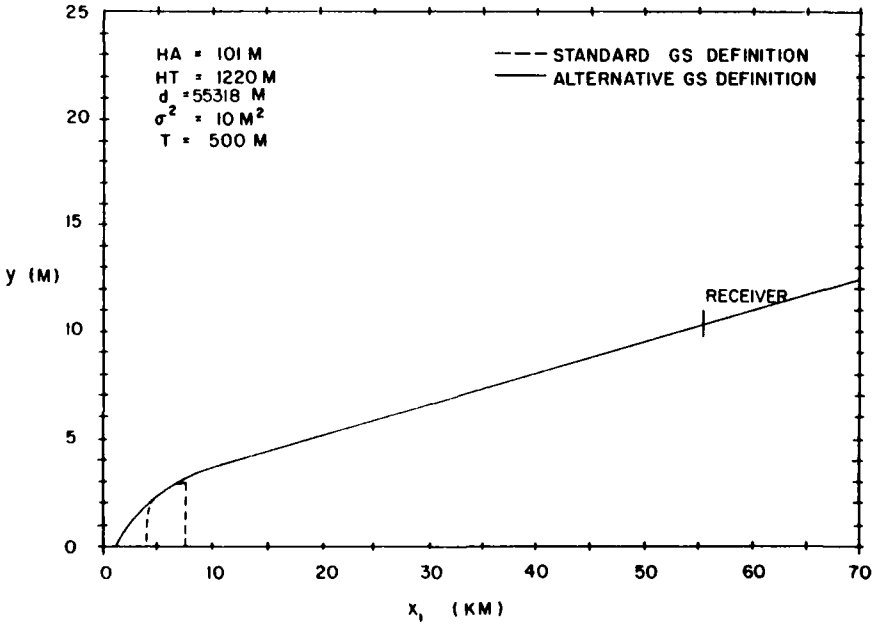

Figure 6. Glistening Surface Dimensions for Both Definitions, Intermediate Antenna Separation, Smooth Surface ($\sigma/T = .006$)

Note that in this derivation, the assumption that $y \ll x_1, x_2$ is still required. This formulation allows us to consider all x_1, x_2 values such that $\not\downarrow 2\beta_o < 90°$ or $\not\downarrow \beta_o < 45° \rightarrow \sigma/T < 0.5$. Before addressing the width assumptions, we can look at some results for the various definitions to clarify the situation discussed so far.

3. CALCULATED SURFACES

In Figure 5 through 15, we will consider three values of β_o and will vary the separation of the antennas from 5 NMI to 30 NMI and then to 50 NMI. This offers us the opportunity to analyze a wide range of conditions. For these cases, the heights are fixed at H_A = 101 m and H_T = 1220 M. This corresponds to heights that we have used in earlier studies, and the implications of those values will be discussed. For this comparison, we consider that the heights are less than the separation, $y < d$, and $y < x_1, x_2$. We will examine the question of height to x_1 and x_2 ratio. From the point of view of the second definition, the selected conditions have $d \rightarrow \infty$ (except possibly the cases where d = 5 NMI).

In Figure 5, we show both sets of results for the boundary of the glistening surface for the case where σ^2 = 10 m^2 and T = 500 m. The roughness is sufficiently small so that the respective antenna heights are always less than the x-distances. At this separation, 50 NMI, the surface given by the first definition extends for half the total distance. The surface obtained from the second definition is in reasonably good agreement out to about x_1 = 30 km. However, since the angle $\not\downarrow \gamma < 1°$, the surface continues to grow indefinitely rather than being cut off, and would have to be terminated by a radar horizon condition. Thus, there is a considerable difference in the surfaces close to the receive antenna.

Figure 6 shows the same case for a separation of 30 NMI. As in the preceding figure, the second definition leads to a continuously growing width. In contrast, for the first definition, the L_1 and L_2 values are almost equivalent to D, and that surface extends only over a short distance near the transmitter. Thus, over most of the separation, the two definitions lead to drastically different results for the predicted glistening surface width.

Figure 7 shows the result for the same conditions when the antenna separation has been reduced to 5 NMI. At that distance, the standard definition results in the combined L_1 and L_2 values exceeding D so that there is no glistening surface. For the second case, if we consider that D = 5 NMI is sufficient to satisfy the condition that $D \rightarrow \infty$, then $\not\downarrow \gamma \approx 8°$. Thus, the first condition on $\not\downarrow \delta$ applies rather than the second, and we obtain a glistening surface of finite extent that is relatively short in length and width, a trend consistent with the nonexistent surface result of the first definition.

$$\gamma - 2\beta_o < \delta < \gamma + 2\beta_o$$

$$0 < \delta \; \pi/2$$

$$-\pi < \alpha < \pi$$

These angular limits are equivalent to:

$$x_1 = H_A \cos\alpha \cot\delta$$

$$y = H_A \sin\alpha \cot\delta$$

It should be noted that the form for Eq. (2) presented here is not the same as the equation given in Section 12.4 of Beckmann and Spizzichino[7] for the case where the transmitter is very far from the receiver. There, the squaring of the sum of sine terms has been omitted.

The difficulty with this approach is that the constraints initially are in terms of angular relations rather than the straightforward (x_1, y) conditions of the preceding case. One of the questions addressed in this report is whether it is reasonable to adopt this more complicated formulism for cases where the height H_T becomes relatively large. The alternative to be considered is the magnitude of the error of the first result when the original assumptions are no longer strictly valid. Associated with this is the reexamination of the (x_1, y) boundary values when those constraints have been relaxed.

To carry out this analysis, we consider the two coordinate limits separately. If we look at the x_1 coordinates of the glistening surface (bounded by L_1, L_2), we see that, as long as β_o is small, all such points satisfy the assumption that $x_1 \gg H_A$ and $x_2 \gg H_T$. As β_o increases, though, some points near the ends of the surface may not satisfy this assumption. The next point is that, if we remove that constraint, we can derive a new expression for the width of the glistening surface that does not require $H_A \ll x_1$ and $H_T \ll x_2$. The result is:

$$y'_{GS} = \pm\left(\frac{x_1 x_2}{d}\right)\left\{\left[\frac{(\sin\gamma_1 + \sin\gamma_2)^2}{\cos\gamma_1 \cos\gamma_2}\right] \mathrm{TAN}^2 \beta_o - \left[\frac{(\cos\gamma_1 - \cos\gamma_2)^2}{\cos\gamma_1 \cos\gamma_2}\right]\right\}^{1/2}$$

where

$$\mathrm{TAN}\ \gamma_1 = \frac{H_A}{x_1} \qquad \text{and TAN}\ \gamma_2 = \frac{H_T}{x_2}$$

Thus, the transmitter is assumed to be located very far from the receiver (see Figure 4).

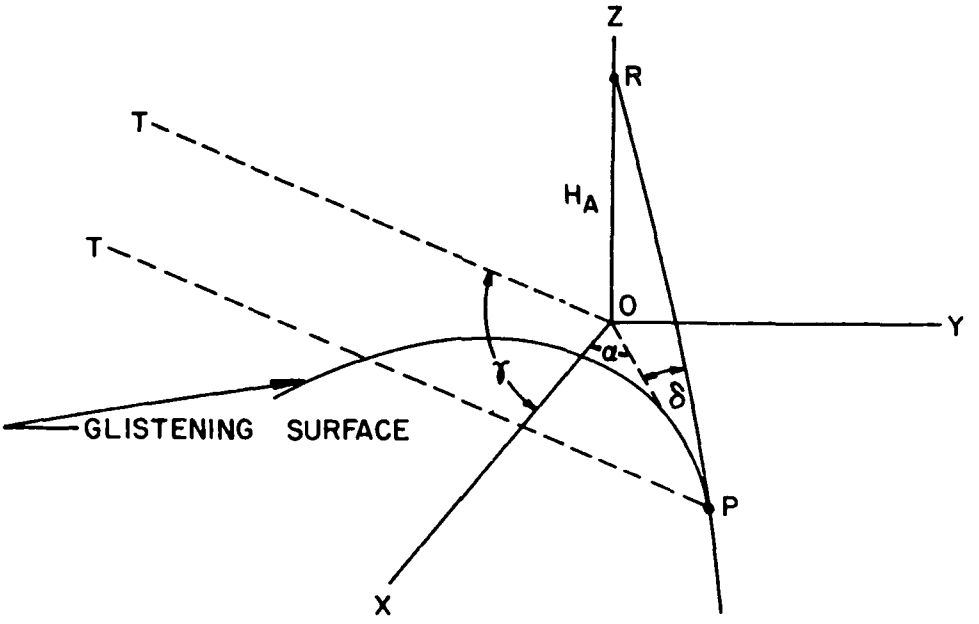

Figure 4. Geometrical Representation of Glistening Surface for System With One Antenna at Infinity

Here again, the equation for the boundary of the glistening surface can be derived by considering the direction cosines of the linear bisector of the angle $\angle RPT$. This line makes an angle β with the z-axis. By expressing the direction cosines of the bisector as a linear combination of the direction cosines of lines PT and PR, setting the angle β equal to β_o, and using the normalization condition for the direction cosines, we can derive the following equation for the boundary of the glistening surface:

$$2\cos\alpha = \left(\frac{\cos\delta}{\cos\gamma}\right) + \left(\frac{\cos\gamma}{\cos\delta}\right) - \mathrm{TAN}^2\beta_o \left[\frac{(\sin\gamma + \sin\delta)^2}{(\cos\gamma \quad \cos\delta)}\right] \tag{2}$$

where the angles α, γ, and δ are defined in Figure 4. For the boundary, $\angle\alpha$ and $\angle\delta$ are confined to the following intervals:

y-coordinate of the boundary of the glistening surface:

$$y_{Gs} = \pm \left(\frac{x_1 x_2}{d}\right)\left[\frac{H_A}{x_1} + \frac{H_T}{x_2}\right]\left[\tan^2\beta_o - 0.25\left(\frac{H_A}{x_1} - \frac{H_T}{x_2}\right)^2\right]^{1/2} \quad (1)$$

For this result, several additional assumptions have been required. These include:

(4) The y-coordinates of the glistening surface boundary are less than x_1 and x_2 that is

$$y \ll x_1,\ x_2$$

where

x_1 = x-coordinate of point on glistening surface boundary,

and

$x_2 = d - x_1$ (see Figure 3);

(5) The angle β_o is small; and

(6) The antenna height, H_A, and the receiver height, H_T, are small compared to x_1 and x_2, that is,

$$H_A \ll x_1 \text{ and } H_T \ll x_2.$$

The effects of these limiting assumptions will be discussed in detail, but first we wish to introduce an alternative definition that Beckmann and Spizzichino[7] derive for slightly different constraints. In this new case, definition 2, assumptions (1) through (3) are still valid, but assumptions (4) through (6) have been replaced by an alternative set of assumptions. For this case, we have:

$$d \to \infty$$

and/or

$$H_T \to \infty$$

isms, as long as some care is used in the application of the conditions of the length determination.

5. DIFFUSE SCATTERED POWER

We have discussed the assumptions and limitations of various glistening surface dimensions for different conditions. To continue our analysis, we turn to the question of how using these different concepts affects the calculated diffuse power scattered from the surface under those conditions.

The basic formalism for the standard calculation is discussed in earlier reports.[1,2,3] We use the centerline σ^o value in the model and assume it applies across the entire width. In their discussion of the second definition, Beckmann and Spizzichino[7] represent the power as a constant term times the integrated area of the surface. In our interpretation of the power scattered by the surface generated by that definition, we again make use of the centerline σ^o distribution and multiply it by the associated width at that point.

In both of these cases, the variation of σ^o with azimuthal angle has been neglected. In order to evaluate the results of the calculations, we carried out the complete analysis in which the actual azimuthal variation of σ^o is included and the power is integrated over the radar footprint for the entire separation rather than the glistening surface. The details of this solution can be found in Papa et al.[5] The distinctive features of these models are summarized in Table 1.

Results for the case $\sigma^2 = 10\,m^2$ and T = 500 m for the exact azimuthally varying σ^o model are shown in Figure 16. The diffuse scattered power in this figure is shown as a function of the separation between the two antennas. For analytical purposes, it should be recalled that the three locations at which glistening surfaces have been examined correspond to 9 km, 55 km, and 92 km. The largest amounts of diffuse scattered power occur at short separations. The power drops sharply out to a distance of 15 km and then tapers off more gradually, decreasing to a level four orders of magnitude below the original levels by a separation of 55 km.

In Figure 17, the standard definition ($2\beta_o$) results are shown for the same roughness factor. At separations less than 52 km, the glistening surface does not exist under this definition, so there is no diffuse power. At greater separations, the power is insensitive to separation.

Figure 18 shows the corresponding variation for diffuse scattered power when the second definition ($d \rightarrow \infty$) is used in the calculation. For separations greater than 55 km, the two results are similar, with the second case exceeding the first by about a factor of two. At shorter separations, though, this definition does not

Table 1. Summary of Scattering Model Cases

Case	Properties
Definition 1	Centerline σ^o H_A, $H_T << X_1$, X_2 $y << X_1$, X_2
Definition 1A	Constraint on H_A, H_T removed
Definition 1B	Constraint removed on H_A, H_T, and Y
Definition 2	Centerline σ^o Separation infinite and/or height of one antenna infinite
Standard of Comparison	σ^o includes azimuthal variation Integration over entire radar footprint

preclude the existence of a glistening surface. Thus, diffuse power is scattered at a fairly constant level until the separation decreases to less than 15 km. There, the power curves show a dip followed by a return to the original levels. Given the similarity in results at larger separations, the question arises as to how the power for the two definitions would agree if the L_1 and L_2 conditions on the original definition surface were relaxed. The scattered power for that case is shown in Figure 19. It is clear that, for separations less than 55 km, this extended length case gives power levels consistent with those of the ($d \longrightarrow \infty$) definition.

Before continuing with general discussions of the models and comparing the results with the more exact case we can use our calculated glistening surface shapes at the three specific separations to interpret the results for the two definitions of glistening surface.

At 55 km, the two results are slightly further apart in power than at 92 km, but, in both instances, the agreement is quite close. This is significant in terms of the depicted surfaces in Figure 6 and Figure 5. In both instances, the difference in dimensions is considerable, particularly at 55 km. To place this in perspective, we have constructed the curves representing the variation in centerline σ^o across the antenna separations as a function of roughness for the three distances discussed in the report. Figure 20 shows the variation for D = 5NMI, Figure 21 is for D = 30 NMI, and Figure 22 corresponds to D = 50 NMI. In these figures, we see that, as the roughness decreases, the value of σ^o begins to be con-

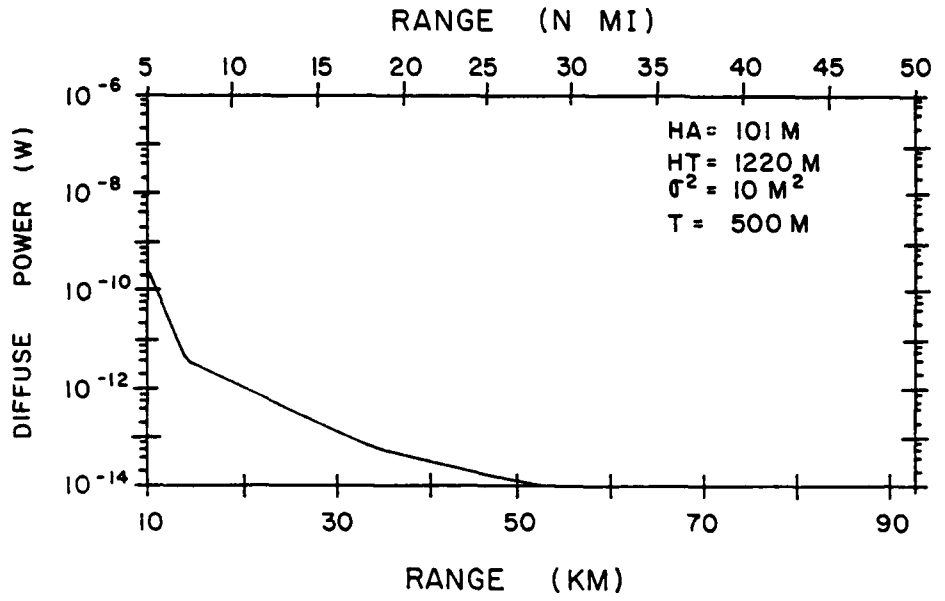

Figure 16. Diffuse Scattered Power as a Function of Antenna Separation, Azimuthal Varying σ^o Calculation, Smooth Surface (σ/T = .006)

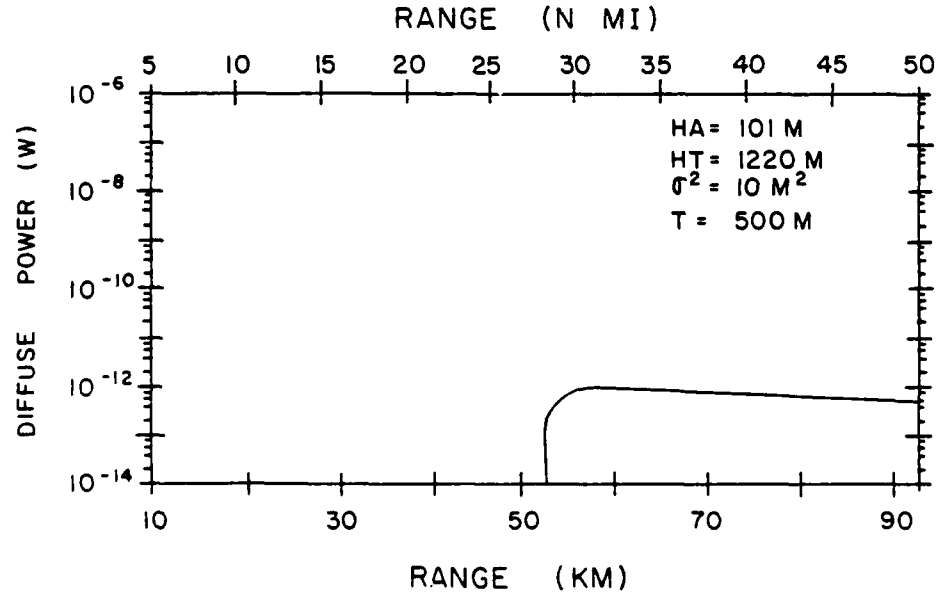

Figure 17. Diffuse Scattered Power as a Function of Antenna Separation, Standard Glistening Surface Calculation, Smooth Surface (σ/T = .006)

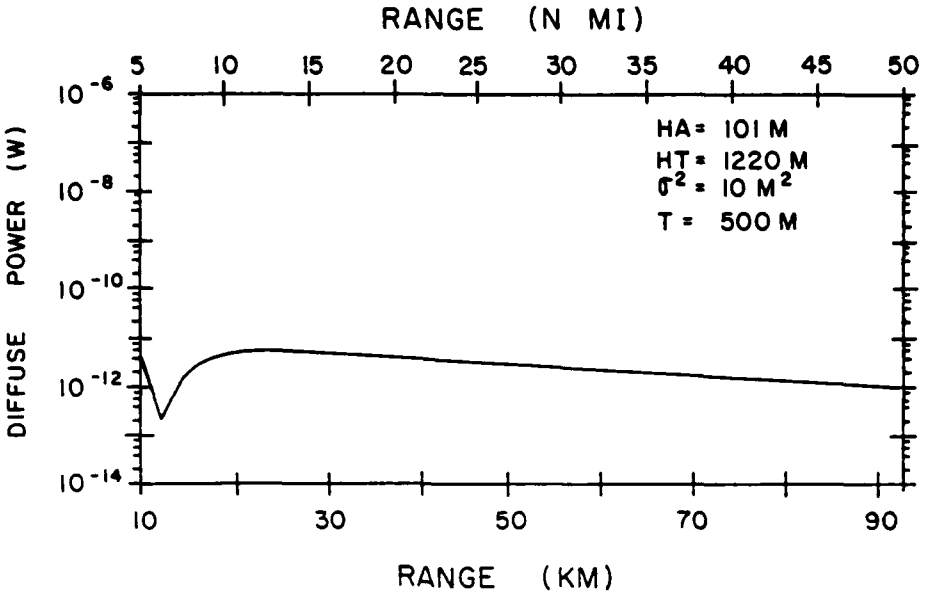

Figure 18. Diffuse Scattered Power as a Function of Antenna Separation, Alternate Definition Glistening Surface Calculation, Smooth Surface (σ/T = .006)

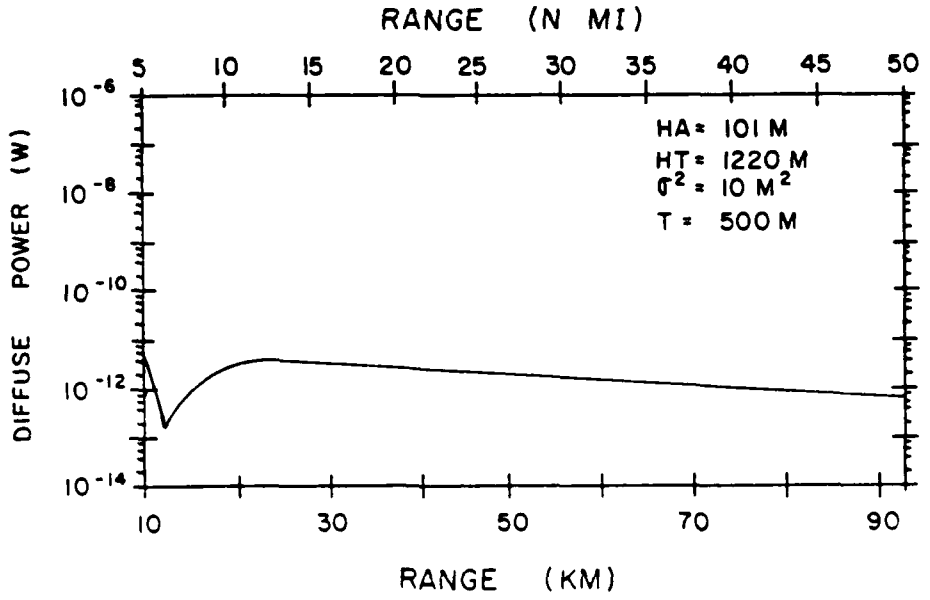

Figure 19. Diffuse Scattered Power as a Function of Antenna Separation, Standard Definition Glistening Surface Without Height Constraints, Smooth Surface (σ/T = .006)

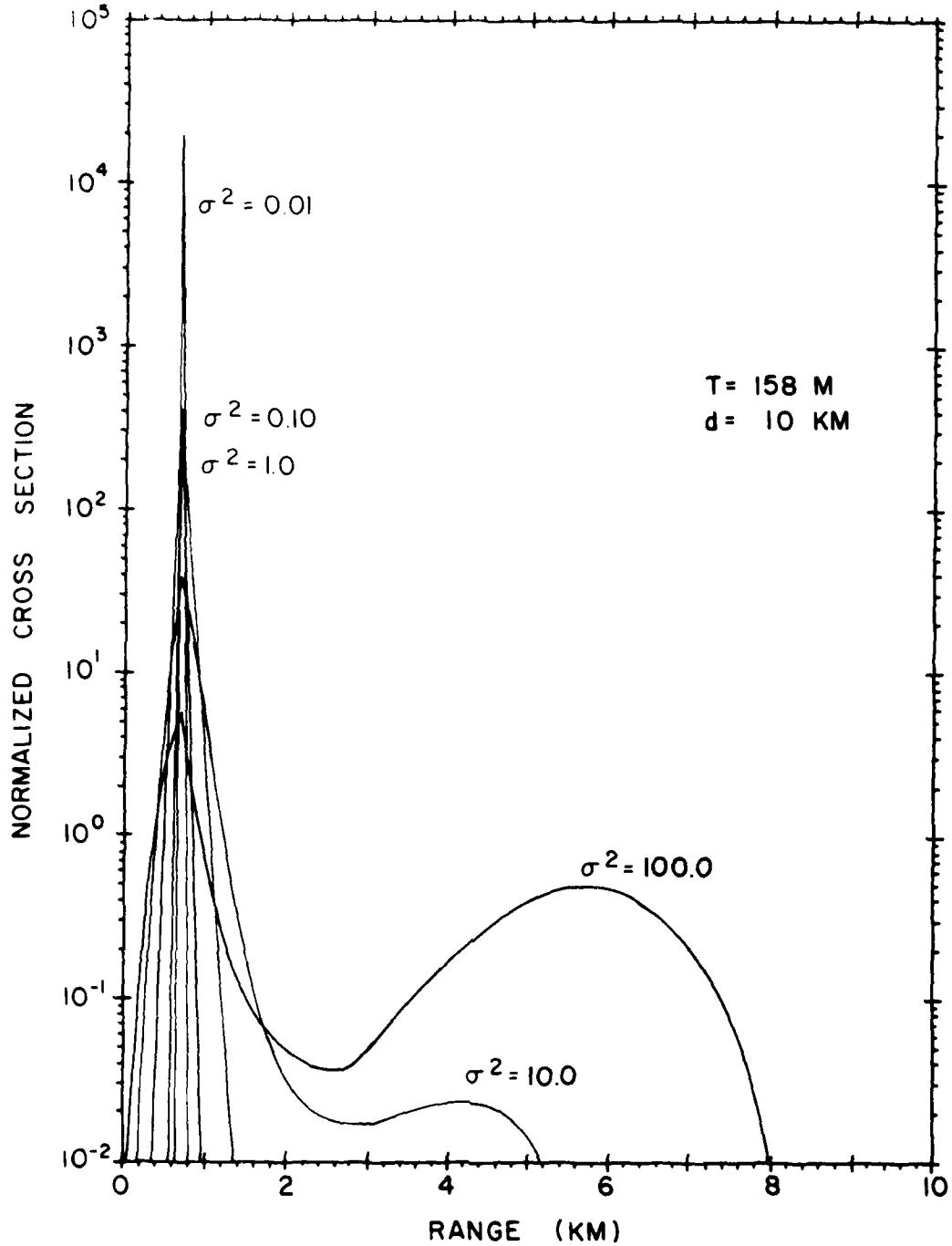

Figure 20. Centerline Variation of of σ^o for Different Roughness Levels, Short Antenna Separation (D = 10 km)

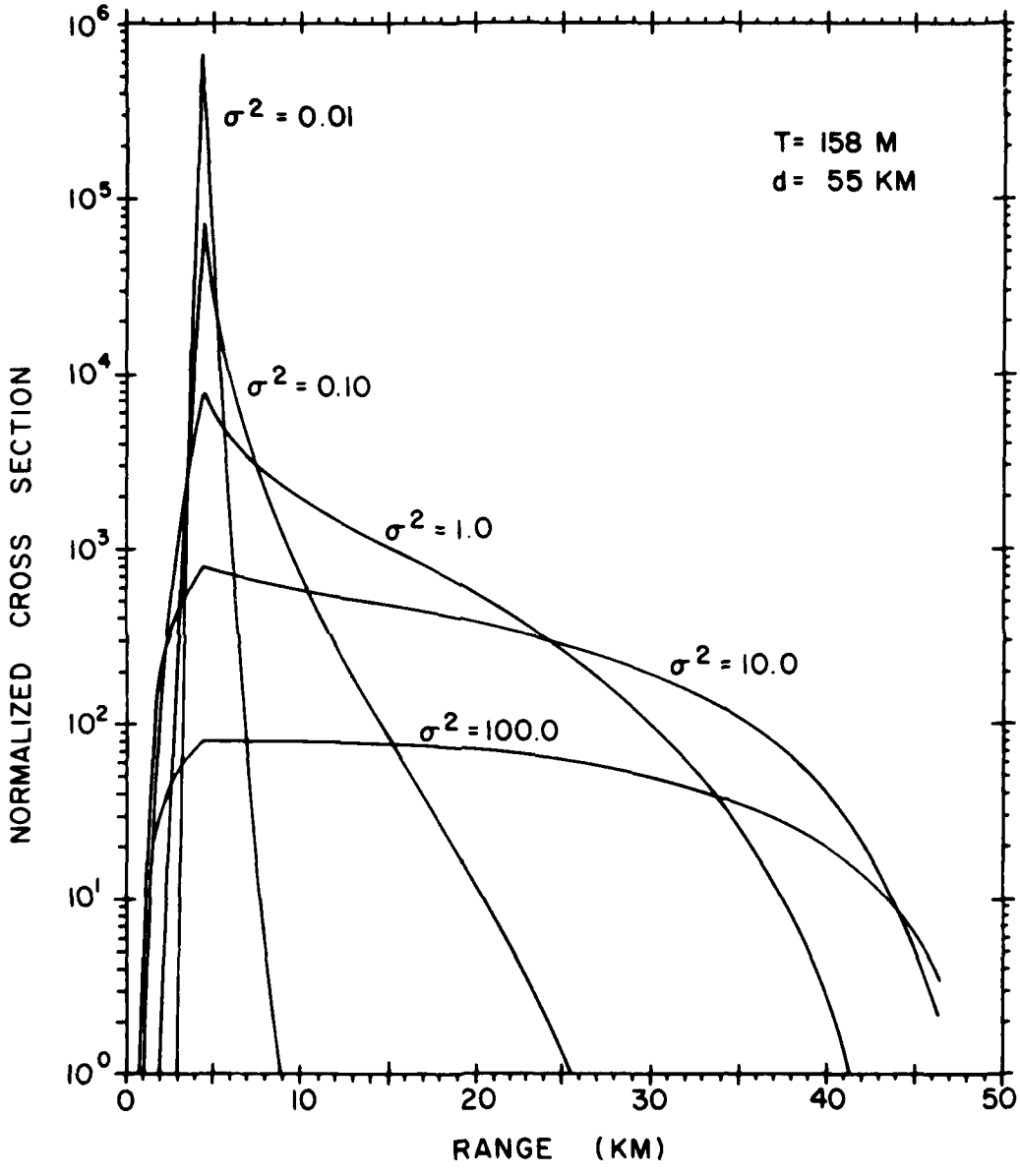

Figure 21. Centerline Variation of σ^o for Different Roughness Levels, Intermediate Antenna Separation (D = 55 km)

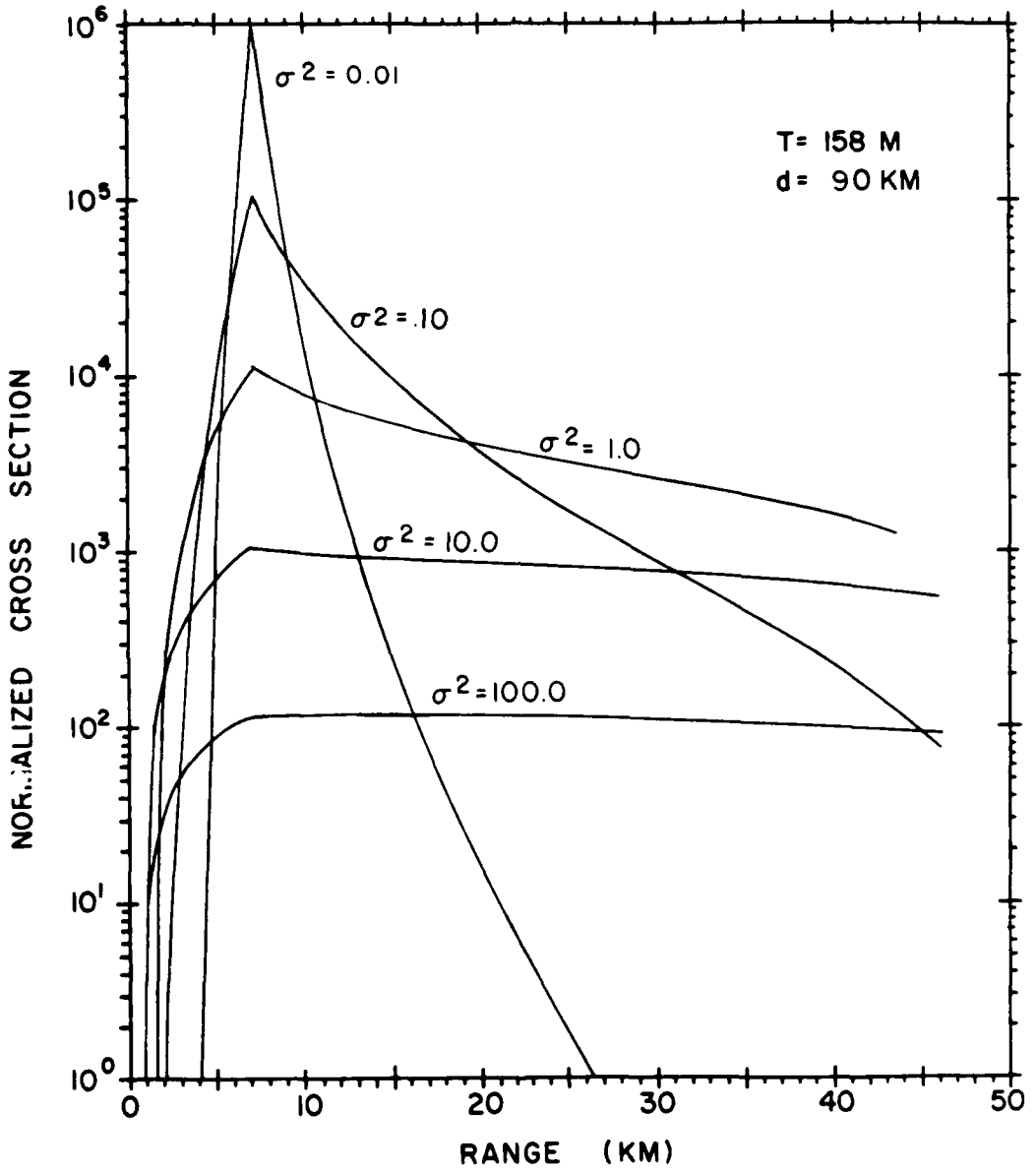

Figure 22. Centerline Variation of σ^o for Different Roughness Levels, Large Antenna Separation (D = 90 km)

fined to a narrow region near the specular point and the peak value becomes sharply higher than for the uniformly distributed σ^o behavior at larger roughness conditions. The case of interest here is that for $\sigma/T = .006$. At 55 km, we see that, by the end of the classical $2\beta_o$ surface, σ^o has dropped to less than half its peak and continues to fall beyond that point. The result is that the two definitions have similar power levels despite the disparity in surface. At 92 km, similar results occur. There, the $2\beta_o$ surface is considerably longer than at 55 km, so the agreement in power levels is even closer. At 9 km, the $2\beta_o$ surface is nonexistent and the alternative surface is the finite ovoid shown. The σ^o variation is not significant in that instance. It should be pointed out, though, that the power for the relaxed length case does agree at that separation. Since the two surface widths are similar at that separation, if L_1 and L_2 are not imposed that result is to be expected.

Now that we have analyzed the behavior of the diffuse scattered power as given by the two glistening surface definitions, we compare those results with the calculated power when the azimuthal variation in σ^o is included in the calculation. The comparisons show that beyond 55 km, where results exist for the two definitions, the result of not including azimuthal σ^o variations is to overestimate the diffuse scattered power by at least two orders of magnitude (20 dB). At shorter separations, we can compare only the second definition solution. We see that the neglect of azimuthal variation gives the result that the power stays relatively constant, while in the correct solution, the value gradually increases. At 15 km, there is a further discrepancy. There, the azimuthal solution rises sharply while the centerline model shows a decrease in power. It should be noted that the solution of Figure 19 also shows a similar pattern at that separation, which is associated with a decrease in the calculated width.

6. CONCLUSION

The conclusion is, first, that the use of centerline σ^o models can lead to calculated diffuse power levels that are in disagreement with the results for the model in which both the azimuthal variation in σ^o is taken into account, and the integration is always across the extent of the radar footprint rather than the calculated glistening surface width.

Secondly, by careful consideration of the length constraints, the basic definition width determination can be used as well as more complicated forms.

Thirdly, even when the assumptions limiting the width have been violated, the results obtained using the basic definition are still quite reasonable. Thus, there is no real justification for introducing the more complicated formalisms for the

determination of the glistening surface width that do not contain the limitations imposed by the original simplifying assumptions.

References

1. Papa, R.J., and Lennon, J.F. (1980) Electromagnetic scattering from rough surfaces based on statistical characterization of the terrain, International Radio Science Symposium (USRI), Quebec, Canada.

2. Papa, R.J., Lennon, J.F., and Taylor, R.L. (1980) Electromagnetic Wave Scattering From Rough Terrain, RADC-TR-80-300, AD A098939.

3. Papa, R.J., Lennon, J.F., and Taylor, R.L. (1982) The Need for an Expanded Definition of Glistening Surface, RADC-TR-82-271, AD A130431.

4. Papa, R.J., and Lennon, J.F. (1983) Investigation of backscatter from an uneven, rough surface, International Radio Science Symposium (URSI), Houston, Texas.

5. Papa, R.J., Lennon, J.F., and Taylor, R.L. (1982) Further Considerations in Models of Rough Surface Scattering, RADC-TR-82-326, AD A130424.

6. Papa, R.J., Lennon, J.F., and Taylor, R.L. (1983) Multipath effects on an azimuthal monopulse system, Trans. IEEE on Aerospace and Electronic Systems, 585-597.

7. Beckmann, P., and Spizzichino, A. (1963) The Scattering of Electromagnetic Waves From Rough Surfaces, Macmillan Co., New York.

8. Ruck, G.T., Barrick, D.E., Stuart, W.D., and Krichbaum, C.K. (1970) Radar Cross Section Handbook, 2, Plenum Press, New York.

9. Long, N.W. (1975) Radar Reflectivity of Land and Sea, Lexington Books, Lexington, Mass.

10. Barton, D.K., and Ward, H.R. (1969) Handbook of Radar Measurement, Prentice-Hall, Inc., Englewood Cliffs, New Jersey.

MISSION
of
Rome Air Development Center

RADC plans and executes research, development, test and selected acquisition programs in support of Command, Control Communications and Intelligence (C^3I) activities. Technical and engineering support within areas of technical competence is provided to ESD Program Offices (POs) and other ESD elements. The principal technical mission areas are communications, electromagnetic guidance and control, surveillance of ground and aerospace objects, intelligence data collection and handling, information system technology, solid state sciences, electromagnetics and electronic reliability, maintainability and compatibility.

Printed by
United States Air Force
Hanscom AFB, Mass. 01731

END

FILMED

7-85

DTIC